Leon Axel, PhD, MD • Ronald M. Summers, BA • Herbert Y. Kressel, MD • Cecil Charles, PhD

Respiratory Effects in Two-Dimensional Fourier Transform MR Imaging[1]

Respiratory and other regular motions during two-dimensional Fourier transform magnetic resonance imaging produce image artifacts consisting of local blurring and more or less regularly spaced "ghost" images propagating along the direction of the phase-encoding magnetic field gradient. The patterns of these ghost artifacts can be understood in terms of the technique of image production and basic properties of the discrete Fourier transform. This understanding permits, without respiratory gating, production of images of improved quality in body regions in which there is significant respiratory motion. In particular, the ghosts can be maximally separated from the primary image by choosing intervals between phase-encoding gradient pulse increments that are equal to one-half the respiratory period; they can be minimally separated by choosing an interval equal to the respiratory period. Increasing the number of signal averages between each phase-encoding increment decreases the intensity of the ghosts.

APPLICATION of magnetic resonance (MR) imaging to regions of the body in which there are significant respiratory motions results in degradation of image quality. Most common MR imaging techniques employ variations of two-dimensional Fourier transform (2DFT) MR imaging in which one direction in space is frequency encoded and an orthogonal direction in space is phase encoded (1, 2). Variations in intensity or position of objects being imaged caused by motion, such as respiratory motion, will result in inconsistencies in MR signals between different signal acquisitions.

The net effect of motion-induced variations in successive signal acquisitions in 2DFT MR imaging techniques of this type is an apparent propagation of artifactual signal along the direction of the phase-encoding gradient (3, 4). When the variation of intensity caused by motion is regular, as in most respiratory motion, the artifactual spread in intensity along the phase-encoded direction may take the form of relatively well-defined "ghost" images or artifacts. These ghost artifacts propagate along the direction of the phase-encoding gradient, independent of the actual direction of the motion causing this artifactual signal. Such ghost artifacts may degrade image quality by obscuring underlying normal or abnormal anatomy and may interfere with quantitative analysis of signal strength from affected regions. Herein, we explain the origin of those motion-induced artifacts, including the spatial relationship of the ghost artifacts to the underlying real anatomy, and we demonstrate means of suppressing the effects of ghost artifact production without using respiratory gating.

BACKGROUND ON 2DFT MR IMAGING

In most techniques of MR imaging, the MR signal is detected in the presence of a magnetic field gradient along a given selected direction (5). The Fourier transform ("spectrum") of the resulting signal is equivalent to a projection of the signal intensity of the object being imaged onto the direction of the magnetic field gradient. The positions of the sources of the signal are thus frequency encoded. An alternative to frequency encoding the position of sources of MR signal is to detect the signal after a pulse of a magnetic field gradient of a given duration and intensity has been applied (1). Applying such a gradient pulse produces a position-dependent phase shift of the signal from positions at different locations along the direction of the magnetic field gradient. The signal is detected repeatedly after a series of different phase-encoding gradient pulses, and an equivalent projection of MR signal intensity along the direction of the magnetic field gradient is then reconstructed from the Fourier transform of the series of detected signals.

Most current clinical MR systems use a hybrid of these two position encoding techniques to reconstruct images (1, 2). The MR signal is detected in the presence of a consistent magnetic field gradient along a given fixed direction, thus producing frequency encoding of position along this direction. However, before each signal detection, a variable pulse of magnetic field gradient is applied in an orthogonal direction. By using a suitable series of variable gradient pulses, the strength of the MR signals will be modulated owing to the phase encoding of signal source position along this gradient in such a way that the position along the direction of the phase-encoding gradient can be recovered by a Fourier transform of the series of signals. A simplified timing diagram of such a pulse sequence is shown in Figure 1.

An image is reconstructed from the resulting series of signals as follows.

The signal strength as a function of time for each successive signal observed in the presence of the frequency-encoding gradient undergoes Fourier transformation to yield the corresponding distribution of signal strength as a function of position along the frequency-encoding gradient. At each frequency, or corresponding position along the frequency-encoding gradient, the signal strengths observed as a function of the strength of the phase-encoding gradient pulse will provide a sequence that also undergoes Fourier transformation to yield the distribution of the signal strength from each position along the phase-encoding gradient at that particular location along the frequency-encoding gradient. Thus, there are two separate Fourier transform steps involved in reconstruction of an image; MR techniques of this type are often referred to as 2DFT MR imaging.

As a result of the differences in the way the image is encoded and reconstructed in the frequency- and phase-encoded directions, variations in intensity of the signals caused by motion during the imaging process will have strikingly different effects on the components of the image along these two different directions. Because the position along the direction of the frequency-encoding gradient is directly recovered by Fourier transformation of the received signal and because the duration of this signal is very brief (typically a few milliseconds), motion along this direction will have only a local corresponding effect in this component direction of the resulting image. Variations in intensity or phase of successive signals, such those caused by motion perpendicular to the section being imaged or motion along the phase-encoded direction, will not have any effect on the frequency-encoded direction in the resulting image. However, the situation is quite different for the component of the image along the phase-encoded direction. Each strip of the image along this direction is reconstructed from the Fourier transform of the sequence of values derived at the corresponding frequency from the series of separate repeated signal acquisitions. The time intervals between these acquisitions may be comparable to the periods of physiologic motions (typically a second or more).

Alterations of the signal sequence caused by motion, which results either in intensity (or phase) variation or physical displacement of objects,
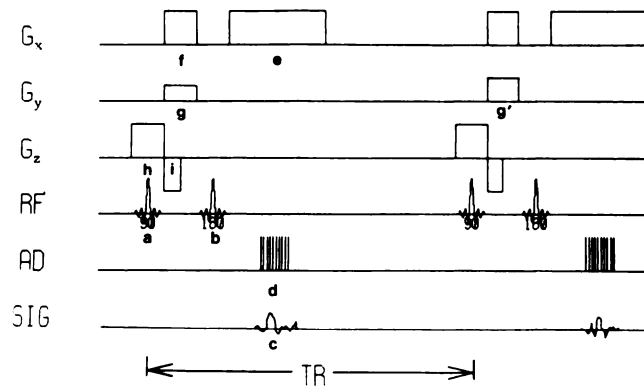

Figure 1. Schematic timing diagram of a 2DFT MR imaging pulse sequence. An initial exciting pulse of radio-frequency (RF) magnetic field (a) produces a 90° rotation of the magnetization of the object being imaged. A subsequent refocusing 180° RF pulse (b) produces a spin-echo signal (c). Signal amplitude is sampled at a set of distinct times (d). The signal is detected in the presence of a frequency-encoding magnetic field gradient (e); the preliminary dephasing pulse of magnetic field gradient (f) provides refocusing of the signal at the time of the spin echo. The phase-encoding magnetic field gradient (g) is applied before detection of the signal in a direction orthogonal to the frequency-encoding gradient. Application of magnetic field gradient pulses (h, i) enables section selection, thus reducing the imaging problem to two dimensions. The pulse sequence is repeated within a repetition time (TR). The frequency-encoding gradient is unchanged in these repetitions, but the phase-encoding gradient pulse (g') will be changed to sample a different Fourier component of the image along its corresponding direction. If a number of signals acquired with a given phase-encoding gradient are acquired and averaged together (NSA) before changing the value of the phase-encoding gradient, the time between different phase-encoding gradients will be given by TR × NSA. G_x, G_y, G_z = magnetic field gradients, AD = amplitude detection, SIG = spin-echo signal.

will result in nonlocal variations in intensity along the phase-encoded direction in the image after Fourier transformation. Any variation in intensity of the sequence will result in corresponding variations in the intensity of the final reconstructed image; in particular, regular, periodic variations in the intensity of the successively acquired signals, such as caused by respiratory motion, will result in corresponding regular variations in space of the intensity of the resulting image (ghost artifacts). See the Appendix for a more detailed discussion of the origin of ghost artifacts and their properties. The higher the frequency of the variations in intensity of the sequence of detected signals, the more widely spaced the corresponding variations of intensity (ghosts) will be in the Fourier transform (image). The greater the amplitude of the intensity variations of the detected signals, the greater the intensity of the ghosts will be.

In practice, one data point in the sequence used in the Fourier transform to reconstruct the image in the phase-encoded direction may be the average of several signal excitations. Thus, the actual time between different phase-encoded signals used in reconstruction is equal to the product of the repetition time (TR) of the pulse sequence times and the number of signals averaged (NSA) for each value of the phase-encoding gradient (TR × NSA); the effective spacing of any regular variations in the sequence of values that will undergo Fourier transformation will depend on both TR and NSA (Fig. 2). For a given TR, as NSA increases so does the total imaging time and thus the number of cycles of the superimposed modulation. We would, therefore, expect the corresponding spacing of ghost artifacts from respiratory motion in actual clinical imaging to depend both on the respiratory rate and its relation to TR and NSA. In particular, we would expect the maximum separation of ghosts from primary images when the respiratory variation was effectively sampled in such a way that successive data points in the sequence to undergo Fourier transformation showed maximum alteration of value. This condition will be fulfilled when the respiratory period is equal to 2(TR × NSA).
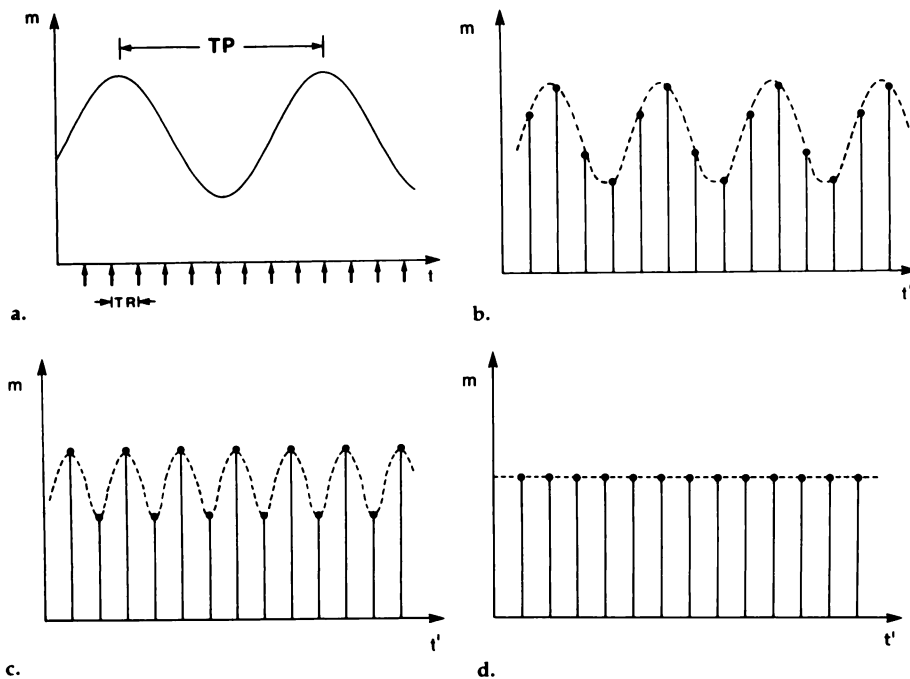
The relationship between ghost ar-

Figure 2. Successive signal acquisitions for reconstruction of the phase-encoded direction effectively sample any superimposed modulation caused by regular motion such as respiration. **(a)** Continuous signal modulation (m) in time (t) caused by repetitive motion with period TP will be sampled by signal acquisitions, symbolized by arrows, at times TR apart. Here, TR = TP/8. **(b)** When a number of signals are averaged together (NSA) for each phase-encoding gradient increment, the effective frequency of the modulation of the successive phase-encoded data will be proportionally increased (the resulting increased total imaging time has a corresponding increased number of cycles of the modulation), and the amplitude of the modulation will be decreased. Here, for the same modulation as in **a**, successive sampled data points are shown as a function of phase-encoding gradient step, t', for NSA = 2. **(c)** As in **b**, with NSA = 4. **(d)** As in **b**, with NSA = 8.

tifacts from regular motions and the frequency of the motion was explored with computer simulations and images of human subjects.

MATERIALS AND METHODS

A computer simulation of MR imaging based on numerical solutions of the Bloch equations for a user-specifiable pulse sequence and distribution of the point objects to be imaged (6) was used to simulate the effects of different kinds of motion when using the general imaging pulse sequence shown in Figure 1. A series of different simulated patterns of motion in both the phase- and frequency-encoded directions relative to the timing of the sequence of increments of values of the phase-encoding gradient was studied.

Healthy volunteers underwent MR imaging in a conventional 1.5-T imaging system (General Electric, Milwaukee). Respiratory rate was monitored by visual observation before the imaging sequence was begun. Different TRs and NSAs were used in imaging the subjects at levels in the chest and upper abdomen. A 2DFT multiplanar interleaved section imaging technique was used, with conventional sequential phase-encoding gradient increments and without respiratory gating.

RESULTS

Figure 3 shows some typical results for simulation studies of the effects

of displacement of the object during the imaging sequence. As previously demonstrated (7), the effects of such displacements on the resulting image are seen to be significantly different along the frequency- and phase-encoded component directions of the image, independent of the actual direction of the motion. The displacement has only a local effect on the frequency-encoded component direction of the image. That is, the actual physical displacement along the direction of the frequency-encoding gradient results in a corresponding blurring of the image in this same direction. However, the effect is rather different along the phase-encoded component direction of the image when the object is moved in either the frequency- or phase-encoded directions. In addition to a local blurring along the direction of the phase-encoding gradient when there is motion in this direction, there is also a nonlocal spread of signal intensity along the direction of the phase-encoding gradient with motion of the object in either direction. The distribution of the intensity along the phase-encoding direction is simply a reflection of the Fourier transform of the pattern of the motion during the

sequence of phase-encoding gradient increments. For a conventional magnitude (phase insensitive) image reconstruction, the distribution pattern of signal intensity spread along the phase-encoded direction depends only on the duration or period of displacement and not significantly on its timing within the sequence of phase-encoding increments. When the displacement of the object is in the phase-encoded direction, the local blurring pattern is superimposed on the broader distribution of intensity along the phase-encoded direction.

When the displacement of the object is regularly repeated, for example, sinusoidal, in either phase- or frequency-encoded directions, it results in a regular modulation of the spread of the intensity along the phase-encoded direction, which gives rise to a regular pattern of ghost artifacts (Fig. 3b–3d). Spacing of ghosts in the final reconstructed images is inversely proportional to the spacing of the pattern of displacements in the sequence of phase-encoding gradient increments (Fig. 3e). Maximum separation of ghosts from primary images is produced with displacements occurring on alternating sequential phase-encoded increments. This will place the ghosts at the edges of the reconstruction region and off the image of the object, if the field of view is suitably larger than the subject. Minimum separation is produced with displacements such that there is only one (or zero, as with gating) cycle of displacement spread over the phase-encoded sequence. This can be approached by suitably choosing the phase-encoding gradient according to the phase of the motion (Fig. 3f). Blurring of the primary image is unchanged by the timing. Increasing the NSA decreases the intensity of the ghost artifacts (Fig. 3g).

As shown by the simulation, randomizing the sequence of phase-encoding gradient increments while keeping the same sequence of displacements of the object and then sorting out of the proper sequence of phase-encoded signals for subsequent Fourier transformation breaks up the regular pattern of ghost artifacts but does not remove the spread of signal intensity along the phase-encoded direction (Fig. 3h).

In images of human subjects at the level of the chest and upper abdomen, regular patterns of ghost artifacts were seen to propagate along the direction of the phase-encoding
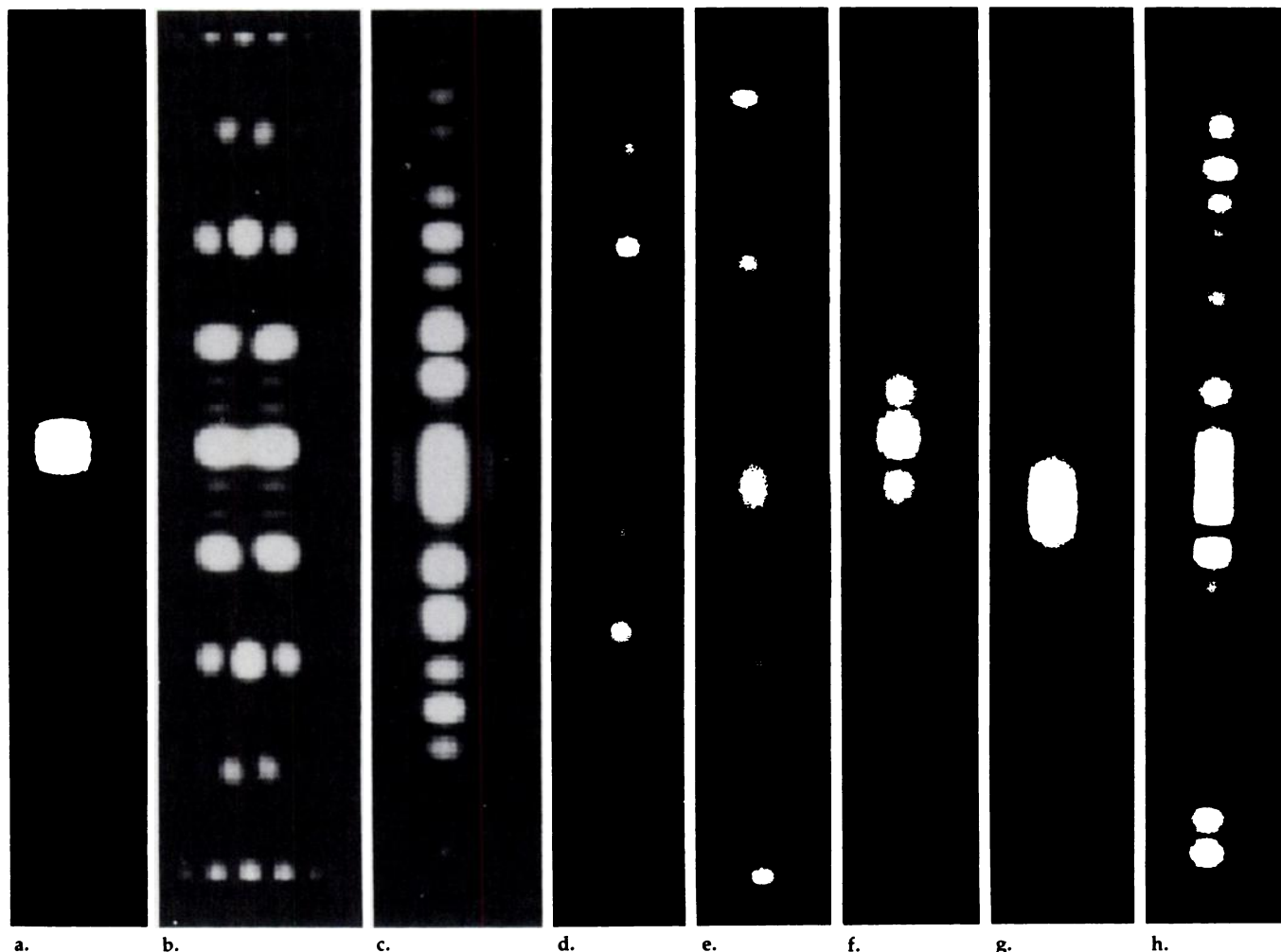
Figure 3. Simulation of motion effects on 2DFT imaging of a point object. (Phase-encoding gradient in vertical direction; data acquisition matrix 32 × 32; displayed as 128 × 128 pixel image.) **(a)** Stationary object. **(b)** Sinusoidal motion (3.9 cycles in imaging time) in frequency-encoded direction. **(c)** As in **b**, but motion in phase-encoded direction. **(d)** As in **c**, but motion perpendicular to imaging plane. **(e)** As in **c**, but motion at twice the frequency. **(f)** As in **c**, but with phase-encoding step chosen by phase of motion to spread one full cycle of motion over the phase-encoding sequence. **(g)** As in **c**, but with increased NSA. **(h)** As in **c**, but with randomized sequence of phase-encoding steps.

gradient (Figs. 4, 5). The strong signal from subcutaneous fat was particularly apparent in the displaced artifacts. For a supine subject, the anterior chest or abdominal wall created the strongest ghost artifact. The more regular the breathing pattern of the subject, the more clearly defined the ghosts were. As demonstrated in Figure 4, the spacing of the artifacts relative to the primary image of the body depended on the TR of the imaging pulse sequence. For a fixed NSA for each phase-encoding gradient increment, with increasing TR, the ghost artifacts were increasingly displaced from the image of the body, up to a maximum when the product of TR and NSA equaled one-half the respiratory period (TP). When the product equaled TP, the ghosts collapsed back onto the primary image. It can also be noted that with increasing TR there was decreased contrast in the resulting primary image because of the decreased effect of differences in tissue T1 relaxation time. The effect of varying the NSA used for each phase-encoding gradient increment while keeping a fixed TR can be seen in Figure 5. Displacement of the ghosts from the primary image is seen to increase with the NSA for a fixed TR. In addition, we note that the image contrast caused by variations in T1 relaxation time is not affected by increasing NSA. The intensity of the ghosts relative to the primary image is decreased when the NSA is greater. The signal-to-noise ratio (S/N) will increase as the square root of NSA.

DISCUSSION

Many factors contribute to the final MR image quality. In addition to the relationship of pulse sequences to tissue relaxation times in determination of image contrast and the relationship of imaging time and choice of spatial resolution to the resulting S/N, motion artifacts are undoubtedly a major factor affecting the quality of images of the chest and abdomen. Although gating (i.e., synchronization of the imaging pulse sequence with the regular physiologic motions of respiration or cardiac contraction so that signals are observed during a particular phase of the motion) can greatly reduce artifacts caused by physiologic motions (8–11), it also may increase the imaging time by reducing the fraction of the time available for data acquisition and can pose technical problems in adjusting the necessary transducers of the physiologic motions to produce proper synchronization. Gating also reduces the flexibility of choice of TRs and thus the amount of T1 weighting in the resulting image. Thus, improved understanding of the origins of artifacts associated with regular motions, which could be used to develop ways to suppress these effects without gating, could have a major impact on the usefulness of MR imaging of the
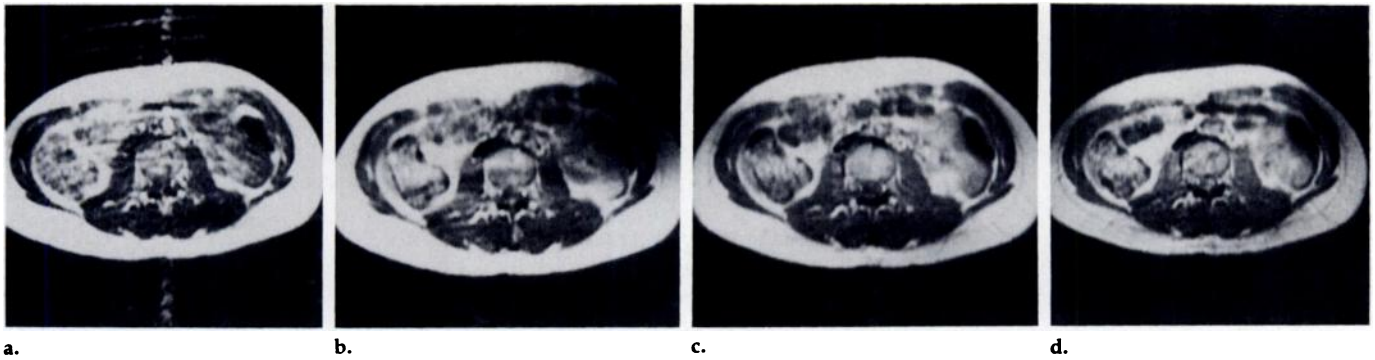
Figure 4. Transverse images of lower abdomen of a healthy subject with a TP of 4 seconds obtained at different TRs (phase-encoding gradient in vertical direction; all with NSA = 2, echo time [TE] = 25 msec). **(a)** TR = 250 msec. **(b)** TR = 500 msec. **(c)** TR = 1,000 msec. The ghost artifacts are displaced by one-half the diameter of the reconstruction region, which in this case is enough to remove them from the image of the body. **(d)** TR = 2,000 msec. The ghosts are now collapsed back onto the original image.

Figure 5. Images of upper abdomen of a healthy subject with a TP of 8 seconds obtained with increasing NSAs (all with TR = 400 msec, TE = 25 msec). **(a)** NSA = 2. **(b)** NSA = 4. **(c)** NSA = 6.

chest and abdomen.

For the commonly used sort of 2DFT MR imaging considered here, the asymmetrical behavior of motion artifacts in the images can be understood in terms of the different ways that position information is encoded along the different directions in the image. In particular, the phase-encoded direction is reconstructed from a sequence of measurements of the signal "samples," which are relatively widely spaced in time. Regular periodic motion during the times between phase-encoding gradient increments results in regularly spaced ghost artifacts displaced along the phase-encoded direction in the image. The spacing of the ghost artifacts is inversely proportional to the interval of the variations of the signal in the sequence of successive phase-encoded samples. Thus, the maximum separation between the primary image of the object and its ghost should come from a timing condition such that the physiologic motion produces maximum variation between sequential phase-encoded samples. That is, for a respiratory period, TP, we would expect a TR to produce the maximum separation of ghost artifacts when it is equal to TP/

(2 × NSA), where NSA is the number of signals averaged per increment of the phase-encoding gradient (the total time between phase-encoding gradient increments is equal to TR × NSA). For a given number of phase-encoding gradient increments, this results in a fixed total optimum imaging time for maximum separation of ghosts from the original moving object, equal to TP/2 times the number of phase-encoding steps.

An alternative optimum imaging condition is to choose the product TR × NSA to be equal to TP. In this case, the variation between sequential phase-encoded samples is minimized and thus the separation of the ghosts from the primary image is also minimized (the ghosts are collapsed back onto the primary image.) However, this technique requires twice as much imaging time as the last one, as each phase-encoding gradient increment takes one TP.

Within the optimum total imaging times defined above, which are determined by the product TR × NSA, there are still trade-offs to be considered in the choice of the relative values of TR and NSA to give a net value of their product. Choosing values of TR less than or equal to the aver-

age tissue T1 relaxation time will result in a relative increase in the contribution of regional differences in T1 relaxation time to the final image contrast. On the other hand, if it is desired to decrease the effects of T1 differences (e.g., so as to increase the relative contribution of regional differences of T2 relaxation time to image contrast), it will be necessary to choose longer values for TR. For values of TR much greater than T1, increasing TR will not significantly increase the S/N in the image. Increasing NSA will increase the S/N in a manner proportional to the square root of NSA. An additional important advantage to increasing the value of NSA is that averaging multiple signals at a given phase-encoding gradient increment results in a net decrease in the variation of the signal at each phase-encoding increment and thus a net decrease in the amplitude of the ghost artifacts at a given spacing of these ghosts.

For these investigations, respiratory rate was monitored by visual observation. However, it could also be monitored by any of the devices used for respiratory gating. The amplitude of the MR signals themselves, when observed without the phase-encod-

ing gradient, will vary with respiration; the pattern of variation of a series of such signals obtained before imaging will permit estimation of the respiratory rate. Because the above techniques assume a fixed value for the respiratory rate, they will be more successful in those subjects with more regular respiratory patterns.

Decreasing the intensity of the ghost artifacts by decreasing the amplitude of the respiratory effects on the signals can be done independently of varying the spacing of the ghosts. As mentioned above, increasing NSA will decrease the intensity of the ghosts by smoothing out respiratory variations. Increasing section thickness will decrease the effect of respiratory motion at right angles to the plane of the section that can move structures in and out of the imaging region. Suppressing the signal from fat, such as with inversion-recovery imaging with T1 chosen to be equal to T_0 for fat (12) or with chemical shift selective saturation pulses (13), will suppress ghost artifacts arising from fat in the body wall. A spatially selective excitation technique that avoids signal from the moving body wall will similarly suppress ghosts arising from it (14). Keeping the TE short will reduce intensity changes caused by phase shifts produced by motion along magnetic field gradients.

In cases in which motion is confined to one portion of the image away from the region of interest, for example, for imaging of the spine, the phase-encoded direction can be chosen to lie along the plane separating the moving and stationary regions so that motion artifacts will not be propagated into the stationary region.

An alternative approach to suppress motion artifacts is to randomize the sequence in which phase-encoded data are acquired. This would smear out or break up the ghosts, although there would still be a net spread of intensity across the image in the phase-encoded direction. Although this approach requires a modified imaging sequence, it does not require respiratory monitoring, and it allows complete flexibility in choice of imaging times.

A final alternative strategy to suppress respiratory effects in 2DFT MR imaging is to minimize the separation of ghost and real images by making the effective "period" of the respiratory variation in the sequence of phase-encoded signals equal to the

duration of the whole sequence without restricting the choice of TR. To accomplish this, the respiratory motion must be monitored by a transducer such as that used for respiratory gating. Alternatively, a small flip angle excitation with a frequency-encoded nonimaging detection of the projection along the direction of maximum respiratory excursion could be inserted between the imaging excitations to monitor the respiratory motion during the scan without the need for external transducers. However, instead of acquiring successively incremented phase-encoded signals at a given phase or specific range of phases of the respiratory cycle as in conventional respiratory gating, in this case we would acquire signals at any arbitrary repetition rate but would apply a suitable phase-encoding increment, depending on the phase of the respiratory cycle at the time of each excitation (15). As the required set of phase-encoded data gets filled up, the nearest (in the sense of respiratory phase) "missing" phase-encoded data set would be acquired. In this way, the final set of phase-encoded data will have corresponding respiratory phases that spread over one full cycle (or one half-cycle, mixing equal degrees of expansion, whether inspiration or expiration) across the set. This technique requires a flexible data acquisition system and a means of monitoring respiration but allows complete flexibility of choice of imaging times and does not prolong the image acquisition time.

The above techniques will reduce the effects of ghost artifacts in the images but will not remove local blurring caused by motion. The use of sufficiently rapid imaging techniques to permit image acquisition during suspended respiration will eliminate all motion artifacts, but at the cost of reduced S/N. This can be compensated for, in part, by averaging repeated images of the same region at the cost of increased imaging time. The use of respiratory gating to acquire signals only during a selected phase of the respiratory cycle can also eliminate motion artifacts. However, signal excitation must be maintained at the same frequency even when data are not being acquired so that the spin saturation is maintained at a steady state. Otherwise, the resulting variation in signal intensity will produce artifacts comparable to those from motion (9).

While we have concentrated on respiratory motion effects here, the

variable intensity effects of pulsatile blood flow can lead to completely analogous effects when imaging blood vessels or the heart, with ghost artifacts propagating along the phase-encoding direction. Similar strategies could be used to reduce the effects of these artifacts by taking into account the relationship of the imaging sequence to the frequency or phase of the cardiac cycle or by increasing NSA, without requiring gating of the acquisition sequence.

In conclusion, with conventional 2DFT MR imaging with sequential phase-encoding increments, the approximate optimum choice of imaging times to maximally separate motion artifacts from the primary image would be for the product of NSA per phase-encoding gradient and TR of the pulse sequence to be equal to one-half of TP. When this product equals TP, the ghosts will be minimally separated from the primary image. The amplitude of the ghost artifacts will be minimized by increasing NSA per phase-encoded increment (as well as by any other means of reducing the amplitude of the respiratory-induced signal variations); the resulting shorter TR needed to keep the above product constant will also increase the relative T1 contrast in the image. Minimizing the effective frequency of respiratory variation in the sequence of phase-encoded data by choosing the value of phase-encoding gradient to be applied according to the phase of the respiratory cycle will minimize the separation of the ghosts from the primary image. Randomizing the sequence of acquisition of phase-encoded signals will break up the ghosts but will not eliminate the spread of intensity along the phase-encoded direction.

APPENDIX

The effects of motion on 2DFT imaging have been rigorously developed for the case of sinusoidal motion (7). We present the basic results in a somewhat less formal way by drawing on well-known properties for Fourier transforms (16) to provide a background for considering ways to reduce the resulting artifacts.

The effect of motion of a point or a coherently moving region in the body being imaged is to modulate the intensity (or phase) of the signal from that region. The modulation function $m(t')$ is given by $m(t') = s'(t')/s(t') = 1 + d(t')$, where t' is the variable equivalent to position within the sequence of phase-encoded signal values, $s(t')$ is the sequence of signal values obtained in the absence of motion, $s'(t')$ is the sequence of signals observed in the presence of motion, and $d(t')$ is propor-
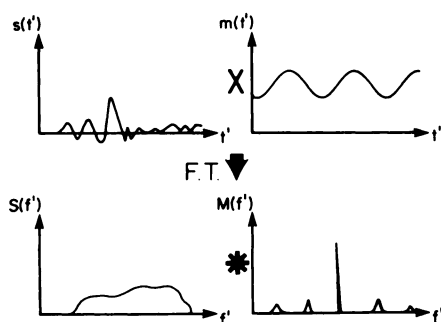
Figure 6. The effect of modulating the sequence of signals from a stationary object acquired with different phase-encoding gradient pulses, s(t'), by a motion-induced variation in signal strength, m(t'), is equivalent to the convolution of the corresponding component of the image of the stationary object along the phase-encoded direction, S(f'), with the Fourier transform (FT) of the modulating function, M(f'). X symbolizes the multiplication of the two functions at the top of the figure; * symbolizes the convolution of their Fourier transforms, at the bottom.

tional to the change in the signal produced by the motion.

The Fourier transform of the observed signal will yield the phase-encoded component of the image. If the Fourier transform of the signal in the absence of motion is $S(f')$ and the Fourier transform of the signal in the presence of motion is $S'(f')$, by the convolution theorem, $S'(f')$ is equal to the convolution of $S(f')$ with the Fourier transform of the modulating function, $M(f') = \delta(f') + D(f')$, where $\delta(f')$ is the Dirac delta function and $D(f')$ is the Fourier transform of $d(t')$. If $d(t')$ is periodic with fundamental period T', $D(f')$ will show "spikes" with spacing proportional to $1/T'$ (Fig. 6). Thus, the image in the presence of motion would be expected to be the sum of the original image plus regularly spaced ghost artifacts in the phase-encoded direction.

By the scaling property of the Fourier transform, the spacing of the ghosts is inversely proportional to the "spacing" of the motion-induced modulations of the signals in the phase-encoded "pseudotime" dimension. Because image reconstruction is performed using the discrete

Fourier transform, those ghosts that would extend beyond the edge of the reconstructed image will be aliased back into the image. The maximum spacing (in f') of the ghosts from the primary image will be seen when the spacing of the modulations in t' is minimal, that is, when the modulation period is equal to two times the interval between samples in pseudotime. Thus, choosing the product TR × NSA to be equal to one-half of TP will provide the maximum spacing of the ghosts from the image.

Conversely, the minimum spacing of the ghosts from the original image will be found when the period of the modulation function in t' is maximum. If one uses scanning techniques fast enough to permit suspended respiration or gates the data acquisition to acquire signals only during the relatively stationary phases of the respiratory cycle, the modulation period is maximized (effectively infinite), and the amplitude of the modulation is minimized, thus essentially eliminating ghosts. Similarly, choosing the product TR × NSA to be equal to TP will provide the minimum spacing of the ghosts from the image in conventional "slow" or ungated imaging. Alternatively, by choosing which sample of pseudotime to acquire (i.e., which phase-encoding gradient pulse to apply) according to the phase of the respiratory cycle, one can maximize the period of the modulating function and minimize ghost spacing without restricting data acquisition to any particular phase of the respiratory cycle.

By Parseval's equation, the intensity of the ghosts will depend on the amplitude of the modulating function. Thus, any means of reducing the amplitude of the modulation, such as increasing NSA, increasing section thickness, decreasing TE, or suppressing the intensity of moving structures, will reduce the intensity of the ghosts independent of any means of changing their spacing. ■

References

1. Kumar A, Welti D, Ernst RR. NMR Fourier zeugmatography. J Magn Reson 1975; 18:69–83.
2. Edelstein WA, Hutchinson JMS, Johnson G, Redpath T. Spin warp NMR imaging and applications to human whole body imaging. Phys Med Biol 1980; 25:751–756.
3. Kundel HL, Kressel HY, Thickman D, Axel L. Motion produces y-direction ghost artifacts in NMR spin-warp imaging (abstr.). Magn Reson Med 1984; 2:189.
4. Schultz CL, Alfidi RJ, Nelson AD, Kopiwoda SY, Clampitt ME. Effect of motion on two-dimensional Fourier transformation magnetic resonance images. Radiology 1984; 152:117–121.
5. Lauterbur PC. Image formation by induced local interactions: examples employing nuclear magnetic resonance. Nature 1973; 242:190–191.
6. Summers RM, Axel L, Israel S. Computer simulation for nuclear magnetic resonance imaging. Magn Reson Med 1986; 3:363–376.
7. Wood ML, Henkelman RM. MR image artifacts from periodic motion. Med Phys 1985; 12:143–151.
8. Runge VM, Clanton JA, Partain CL, James AE. Respiratory gating in magnetic resonance imaging at 0.5 Tesla. Radiology 1984; 151:521–523.
9. Ehman RL, McNamara MT, Pallack M, Hricak H, Higgins CB. Magnetic resonance imaging with respiratory gating: techniques and applications. AJR 1984; 143:1175–1182.
10. Lanzer P, Botvinick EH, Schiller NB, et al. Cardiac imaging using gated magnetic resonance. Radiology 1984; 150:121–127.
11. Go RT, MacIntyre WJ, Yeung HN, et al. Volume and planar gated cardiac magnetic resonance imaging: a correlative study of normal anatomy with thallium-201 SPECT and cadaver sections. Radiology 1984; 150:129–135.
12. Bydder GM, Young IR. MR imaging: clinical use of the inversion recovery sequence. J Comput Assist Tomogr 1985; 4:659–675.
13. Bottomley PA, Foster TH, Leue WM. Chemical imaging of the brain by NMR. Lancet 1984; 1:1120.
14. Feinberg DA, Hoenninger JC, Crooks LE, Kaufman L, Watts JC, Arakawa M. Inner volume MR imaging: technical concepts and their applications. Radiology 1985; 156:743–747.
15. Bailes DR, Gilderdale DJ, Bydder GM, Collins AG, Firmin DN. Respiratory ordered phase encoding (ROPE): a method for reducing respiratory motion artifacts in MR imaging. J Comput Assist Tomogr 1985; 4:835–838.
16. Bracewell RN. The Fourier transform and its applications. 2d ed. New York: McGraw-Hill, 1978.